Development of a Mathematical Model for the Simulation of a Non-Agitated Ice Slurry Storage Tank

Justin Tamasauskas[1], Michel Poirier[1], Radu Zmeureanu[2], and Roberto Sunyé[1]
[1] CanmetENERGY, Natural Resources Canada, Varennes, Qc
[2] Dept. of Building, Civil & Environmental Engineering, Concordia University, Montreal, Qc

Abstract

This paper presents a new model of a non-agitated ice slurry storage tank. Modelling is based on energy balances applied to separate ice and water layers. The defining equations are then discretized and used as a base for a new component for the TRNSYS energy simulation program. A comparison of the new component model with measured data confirms its ability to predict the ice mass and tank fluid temperature in both the ice building and ice melting modes of operation.

1 Introduction

Renewable energy technologies such as solar collectors and heat pump systems play an important role in reducing residential energy use. In particular, the use of a solar assisted heat pump system has been shown to significantly reduce the energy used for heating and hot water preparation purposes (Freeman et al, 1978). Solar systems often require thermal storage to bridge the time discrepancy between thermal supply and demand. The majority of solar systems use some form of sensible storage, which can impose significant space requirements within the building. Latent storage systems use the latent heat available during the melting or solidification of a Phase Change Material (PCM) to store energy at a higher density (Hasnain, 1998).

Ice as a Latent Storage Material

Using ice as a storage material offers a number of potential benefits in residential applications. First, the latent heat of ice is higher than for a number of other commonly used PCMs (Hawes et al, 1993), allowing for higher energy storage densities and reduced tank volumes. Ice/water is also a naturally occurring substance, allowing for a low cost and environmentally friendly storage material.

Several methods of ice generation have been examined in the literature. A large number of ice storage applications use an ice-on-coil design, where the evaporator coils of a heat pump are placed directly in the storage tank (ASHRAE, 2007). These systems often experience degraded performance due to the added thermal resistance of the ice. Locating the coils within the tank also reduces the available storage volume. Ice slurry (a mixture of small diameter ice particles and water (IIR, 2005)) offers an alternative to these issues by separating the storage and ice generation equipment. In addition, ice slurry also has the ability to absorb large amounts of thermal energy because of the increased surface area in the mixture (Ure, 1999).

Ice slurry has a number of applications in residential buildings. During the heating season the slurry mixture can be used as a thermal storage material in order to bridge the time discrepancy between thermal supply and demand. The quality of stored energy can then be upgraded using a heat pump in order to meet the space heating and Domestic Hot Water (DHW) loads of the home (Tamasauskas et al, 2011). Ice slurry can also be used in cooling

applications. In this case slurry from the ice generator is used to maintain the ice tank as a cold storage reservoir. Cold water, or an ice slurry mixture, can then be extracted from the tank and used at a cooling coil inside the home.

Ice Storage in Solar Assisted Heat Pump Systems

Ice storage can be particularly beneficial when used in conjunction with solar thermal collectors. Figure 1 compares the theoretical efficiency of a solar collector (1) operating in series with an ice storage tank, and (2) operating in series with a warm water storage tank (outdoor air temperature set at -5°C). The use of ice storage allows a cold temperature fluid to be circulated in the collector loop, reducing thermal losses to the ambient and allowing for increased thermal gains.

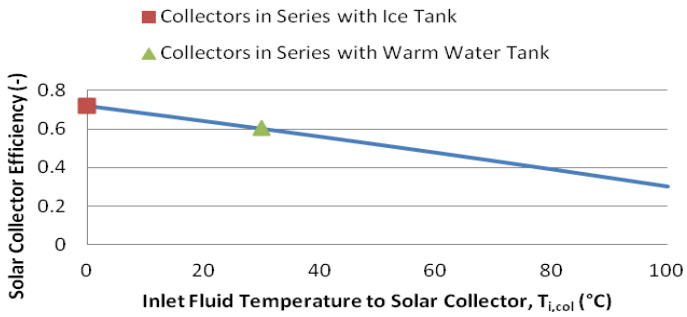

Figure 1- Impact of Ice Storage on Solar Collector Efficiency

A proposed integration of ice storage into a solar assisted heat pump is shown in Figure 2. Ice slurry is generated at the heat pump, and allowed to stratify within a non-agitated ice storage tank. In Solar Loop A, cold water from the bottom of the ice tank is circulated to the collectors, with the quality of thermal energy subsequently upgraded using the heat pump. Solar Loop B allows the collectors to operate directly against the warm water tank when ambient conditions result in the collectors producing fluid at or above the space use temperature.

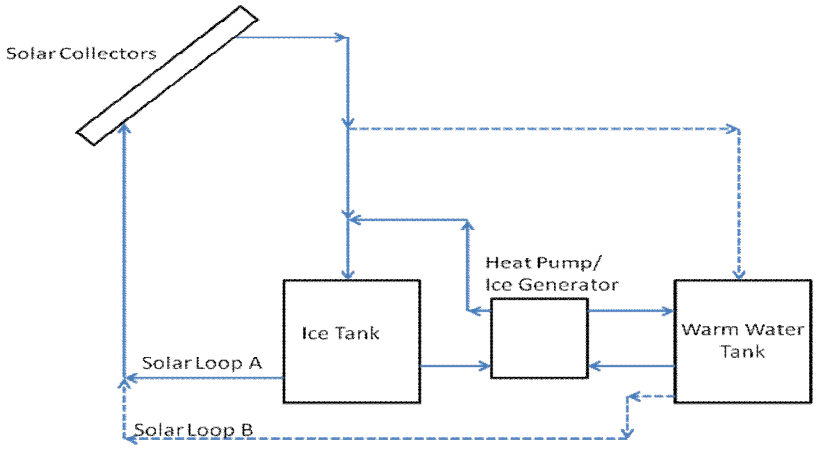

Figure 2- Integration of Ice Storage with Solar Heat Pump System

Modeling of Ice Storage Tanks

Several authors have proposed mathematical models of ice storage tanks operating independently of the ice generating device. Behschnitt (1996) developed a model of an ice tank for the TRNSYS energy simulation program. A single energy balance was applied to the tank, taking into account thermal gains/losses from the incoming flow stream and ambient air. An effectiveness coefficient was used to relate the inlet and outlet fluid temperatures based on the amount of ice remaining at the current time step. While simple and computationally efficient, the model did not directly account for the thermal capacity of the fluid in the tank, leading to large temperature fluctuations under certain operating conditions.

Tanino et al. (2001) took a detailed approach to modeling the performance of an ice slurry storage tank. The model was divided into independent storage and melting modules. The storage section used a series of mass balance equations to examine ice compaction and agglomeration in the radial and axial directions. The melting section of the model used a series of energy balance equations in order to determine the outlet fluid temperature and ice mass at each time step. The lack of energy balance equations in the storage sub-section means that this portion of the model would need to be modified to account for thermal gains or losses due to the incoming flow stream and ambient air, should the model be used in system simulations.

Egolf et al. (2008) developed a model to examine the stratification process inside an ice slurry storage tank. Particle conservation equations were applied to differential mass elements oriented axially in the tank, with each equation taking into account the movement of particles due to diffusion and buoyancy, and the melting/freezing of ice. The model assumed adiabatic conditions at all times, and as such cannot be applied to solar storage systems in which thermal energy is added and extracted via the solar collectors and heat pump.

Based on a review of the available literature, it is concluded that a new ice tank model is required with the following features:

i. Many of the current models are aimed at a detailed examination of specific aspects of tank performance (i.e. ice compaction, or fluid velocity). The new model should focus on calculating the tank fluid temperature and ice mass, as these are the primary requirements for systems level research.
ii. A common theme in many models is the separation of the ice and water nodes. As such, the new model should deal with each node separately.
iii. The current TRNSYS ice tank model does not include a thermal capacitance term for the tank fluid. The new model should include the thermal capacitance of the fluid to make the tank model more widely applicable.

The objective of this paper is to present the development of a new semi-empirical model of an ice slurry storage tank. The proposed model is created for use in systems level research, and, as such, is focused on determining a simple and computationally efficient method of predicting the main indicators of ice tank performance.

2 Mathematical Model

Developing a new ice tank model involves mathematically describing the heat transfer processes in the tank. This section presents the development assumptions and energy balance equations used to create the new ice tank component.

Development Assumptions

i. Ice and water separate into two distinct layers at each time step. Each layer is assumed to consist of a single node, with temperature stratification effects neglected.
ii. Inlet fluid to the tank is introduced as a uniformly distributed spray over the top of the tank.
iii. Sub-cooling of the ice layer is neglected, with the temperature of ice (T_{ice}) set at a constant value of 0ºC.
iv. The ice thickness is independent of the radial distance from the tank axis. The density and porosity of ice are also assumed to be constant throughout the layer.
v. The bottom of the tank is well insulated, and as such heat losses through this section are negligible. Heat losses from the ice layer to the air at the top of the tank are also assumed to be negligible.

Energy Balance Equations

The ice tank is divided into ice and water control volumes, as shown in Figure 3. Energy balance equations are then applied to each control volume.

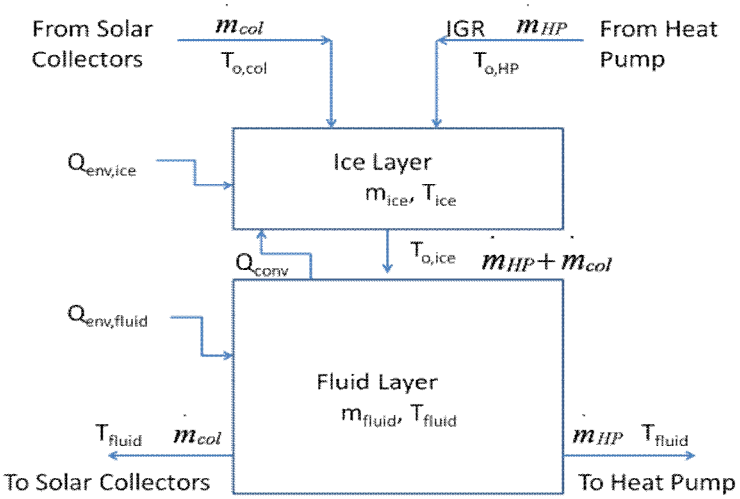

Figure 3- Ice and Water Control Volumes

The energy balance for the ice layer is written as:

$$-L\frac{dm_{ice}}{dt} = \dot{m}_{col}\,c_p\left(T_{o,col}-T_{o,ice}\right)+\dot{m}_{HP}\,c_p\left(T_{o,HP}-T_{o,ice}\right)-IGR\cdot L + UA_{s,ice}\left(T_{env}-T_{ice}\right)+hA_c\left(T_{fluid}-T_{ice}\right) \quad (1)$$

The energy balance for the water layer is written as:

$$m_{fluid}c_p\frac{dT_{fluid}}{dt} = \left(\dot{m}_{HP}+\dot{m}_{col}\right)c_p\left(T_{o,ice}-T_{fluid}\right)+UA_{s,fluid}\left(T_{env}-T_{fluid}\right)-hA_c\left(T_{fluid}-T_{ice}\right) \quad (2)$$

Effectiveness Function Approach

Heat transfer between the incoming flow stream and ice layer is defined using an effectiveness coefficient (Behschnitt, 1996), which relates actual heat transfer to a theoretical maximum heat transfer in which the fluid temperature exiting the ice layer equals the temperature of ice (T_{ice}=0°C):

$$\varepsilon = \frac{\dot{m}_{HP}\, c_p \left(T_{o,HP} - T_{o,ice}\right) + \dot{m}_{col}\, c_p \left(T_{o,col} - T_{o,ice}\right)}{\dot{m}_{HP}\, c_p \left(T_{o,HP} - T_{ice}\right) + \dot{m}_{col}\, c_p \left(T_{o,col} - T_{ice}\right)} \tag{3}$$

The fluid temperature exiting the ice layer ($T_{o,ice}$) is then calculated as follows:

$$T_{o,ice} = \frac{\dot{m}_{col}\, T_{o,col} + \dot{m}_{HP}\, T_{o,HP} - \varepsilon\left(\dot{m}_{HP}\left(T_{o,HP} - T_{ice}\right) + \dot{m}_{col}\left(T_{o,col} - T_{ice}\right)\right)}{\dot{m}_{col} + \dot{m}_{HP}} \tag{4}$$

The effectiveness coefficient (ε) for this study was calculated over a range of ice mass fractions (γ) using experimental data from ASHRAE Report RP707 (ASHRAE, 1993). Three sets of data were used during the development process, with each data set corresponding to a case where the inlet fluid flow was distributed uniformly over the top of the tank as assumed by the mathematical model. Each set of test data was presented in the form of a graph depicting the ice mass and tank fluid temperature over time. The reported experimental fluid temperature was based on the average reading of twelve thermocouples placed along the perimeter outlet of the tank. The FindGraph computer program (UNIPHIZ Lab, 2011) was used to digitize each graph and obtain numerical values of the ice fraction and tank temperature at different points in time. The heat transfer effectiveness at each data point was then calculated based on the assumption that the measured outlet fluid temperature from the tank equaled the fluid temperature exiting the ice layer ($T_{o,ice}$=T_{fluid}):

$$\varepsilon = \frac{\left(T_{o,col} - T_{o,ice}\right)}{\left(T_{o,col} - T_{ice}\right)} = \frac{\left(T_{o,col} - T_{fluid}\right)}{\left(T_{o,col} - T_{ice}\right)} \tag{5}$$

The calculated effectiveness coefficient function is shown in eqn. (6). The equation for the data range 0.02≤γ≤0.44 is based on a fifth order polynomial regression performed using a data set comprising of all three test runs. The resulting coefficient of determination was 0.715. A linear decrease in the effectiveness function is assumed from ε=0.847 at γ=0.02 to ε=0 at γ=0 (Behschnitt, 1996). Above γ=0.44 the effectiveness function is set to its maximum possible value of 1.

$$\varepsilon = \begin{cases} 42.35\gamma & \left|0 \le \gamma < 0.02\right. \\ 121.5\gamma^5 - 165.9\gamma^4 + 88.77\gamma^3 - 23.31\gamma^2 + 3.12\gamma + .7928 & \left|0.02 \le \gamma \le 0.44\right. \\ 1 & \left|0.44 < \gamma \le 1\right. \end{cases} \tag{6}$$

3 Integration of Mathematical Model with TRNSYS

The primary objective of the work presented in this paper is the development of a new ice tank component for use in systems level research. As such, the developed mathematical model was used as a base for a new component (Type 213) for the TRNSYS energy simulation program (Klein et al, 2004).

Discretization of Energy Balance Equations

Each energy balance equation must be discretized to allow TRNSYS to determine the numerical solution to the ice mass (m_{ice}^{t}) and tank fluid temperature (T_{fluid}^{t}) at the end of a time step *t*. For the ice layer, the discretized equation is:

$$-L\frac{\left(m_{ice}^{t}-m_{ice}^{t-1}\right)}{\Delta t}=\begin{pmatrix}\dot{m}_{HP}^{t}\,c_p\left(T_{o,HP}^{t}-T_{o,ice}^{t}\right)+\dot{m}_{col}^{t}\,c_p\left(T_{o,col}^{t}-T_{o,ice}^{t}\right)-IGR^{t}\cdot L\\ +UA_{s,ice}^{t}\left(T_{env}^{t}-T_{ice}\right)+hA_{c}^{t}\left(T_{fluid}^{t-1}-T_{ice}\right)\end{pmatrix} \tag{7}$$

For the water layer the discretized equation is:

$$m_{fluid}^{t}c_p\frac{\left(T_{fluid}^{t}-T_{fluid}^{t-1}\right)}{\Delta t}=\begin{pmatrix}\left(\dot{m}_{HP}^{t}+\dot{m}_{col}^{t}\right)c_p\left(T_{o,ice}^{t}-T_{fluid}^{t-1}\right)\\ +UA_{s,\,fluid}^{t}\left(T_{env}^{t}-T_{fluid}^{t-1}\right)-hA_{c}^{t}\left(T_{fluid}^{t-1}-T_{ice}\right)\end{pmatrix} \tag{8}$$

Iterative Approach

Equations (7) and (8) are solved successively to determine the tank fluid temperature (T_{fluid}^{t}) and ice mass (m_{ice}^{t}) at the end of each time step *t*. However, obtaining a solution to eqn. (8) requires a knowledge of the current fluid mass (m_{fluid}^{t}), which cannot be known without calculating the current ice mass (m_{ice}^{t}) As such, an iterative solution algorithm is used to calculate T_{fluid}^{t} and m_{ice}^{t} at each time step.

At the initial iteration (*n*=0),

1. The fluid mass at time t is set equal to the fluid mass at the end of time step t-1

$$m_{fluid,0}^{t}=m_{fluid}^{t-1} \tag{9}$$

2. Equation (8) is solved to determine the average tank fluid temperature ($T_{fluid,n}^{t}$). This value is then used in eqn. (7) to estimate the ice mass ($m_{ice,n}^{t}$).

At iterations $n\geq 1$,

1. The fluid mass is recalculated based on the ice mass calculated during the previous iteration ($m_{ice,n-1}^{t}$):

$$m_{fluid,n}^{t}=m_{tank}-m_{ice,n-1}^{t} \tag{10}$$

2. Equation (8) is solved to determine the average tank fluid temperature ($T^t_{fluid,n}$). This value is then used in eqn. (7) to determine a new estimate of the ice mass ($m^t_{ice,n}$).
3. The revised estimates of $T^t_{fluid,n}$ and $m^t_{ice,n}$ are compared with those determined at iteration *n-1*. Iterations are terminated when:

$$\left|T^t_{fluid,n} - T^t_{fluid,n-1}\right| \le 0.01°C \tag{11}$$

$$\text{and } \frac{\left|m^t_{ice,n} - m^t_{ice,n-1}\right|}{m^t_{ice,n-1}} \le 0.01 \tag{12}$$

Calculation Assumptions

The following assumptions are used during the calculation procedure:

i. The variables $A^t_{s,ice}$, $A^t_{s,fluid}$, A^t_c, and $T^t_{o,ice}$ (at time step *t*) are all evaluated based on the ice mass at the end of time step *t-1*. If m^{t-1}_{ice} is 0 kg, the contact area between the ice and water layers (A^t_c) is set to 0 m^2.
ii. Values for density and specific heat are based on the tank fluid temperature at time step *t-1*.
iii. Heat transfer between the ice and water layers, and between the water layer and the ambient, is based on the fluid temperature at time step *t-1*.

4 Validation of Simulation Results

The mathematical model is compared with experimental data to ensure that it adequately predicts the ice mass and tank fluid temperatures over time. Two primary operational modes are examined:

i. Charging (ice building) process
ii. Discharging (ice melting) process

Validation of the Charging (Ice Building) Process

Experimental data for the ice charging process was obtained from an ice slurry test bench operating at the CanmetENERGY facility in Varennes, Quebec. The ice storage tank had an inner radius of 0.96 m and a height of 1.23 m. The total tank storage capacity was 632 kg, with an ice storage capacity of 250 kg. All tests were performed using an initial 5% (by mass) ethylene glycol solution.

For each test, fluid was extracted from the bottom of the ice tank and directed to an external ice slurry generator (IGR=0.033 kg/s). Ice slurry exiting the generator was then reintroduced through an opening in the side of the tank. All validation tests were performed with the mechanical stirrer device turned off in order to facilitate the stratification of the ice and water layers as assumed during the development of the mathematical model. The initial fluid temperature in the tank was -1.5°C, while the initial ice mass was 0 kg.

The fluid temperature in the tank was recorded at 15 s intervals using resistance temperature detectors (RTDs, accuracy ± 0.05°C). Experimental ice fractions were determined using a two-step procedure. First, the measured tank fluid temperature was used to determine

the current mass concentration of ethylene glycol in the tank based on the formula (Renaud-Boivin et al, 2012):

$$\lambda_{gly} = -0.0354T_{fluid} - 0.00171T_{fluid}^2 - 0.00007072T_{fluid}^3 - 0.00000163T_{fluid}^4 - 0.00000001488T_{fluid}^5 \quad (13)$$

The current ice concentration (by mass) was then calculated as follows:

$$\gamma = 1 - \frac{\lambda_{gly}^0}{\lambda_{gly}} \quad (14)$$

Simulations were performed in TRNSYS using the developed ice tank model, and above defined tank geometry and test parameters. To allow for an accurate base of comparison, the ice tank model was modified to account for the changing concentration of ethylene glycol over time. For simulation purposes, the ice tank was also assumed to operate solely against the ice generator, with no additional extraction of cold water for other purposes. The temperature of fluid returning to the tank from the ice generator was then varied according to the freeze point of fluid at the current ethylene glycol mass concentration in the tank.

The simulated and experimental ice fractions (by mass) are compared in Figure 4. Both data sets follow a similar trend, with a steady rise in the ice fraction over time. The two data sets experience larger discrepancies after *t*=40 minutes, with a maximum difference of 7% of the tank storage capacity. One possible reason for this difference is temperature stratification within the tank. All experimental ice fractions were determined using eqn. (13), which assumes a well mixed tank. The lack of mechanical agitation during testing may have led to this equation providing less accurate estimates of the current ice mass.

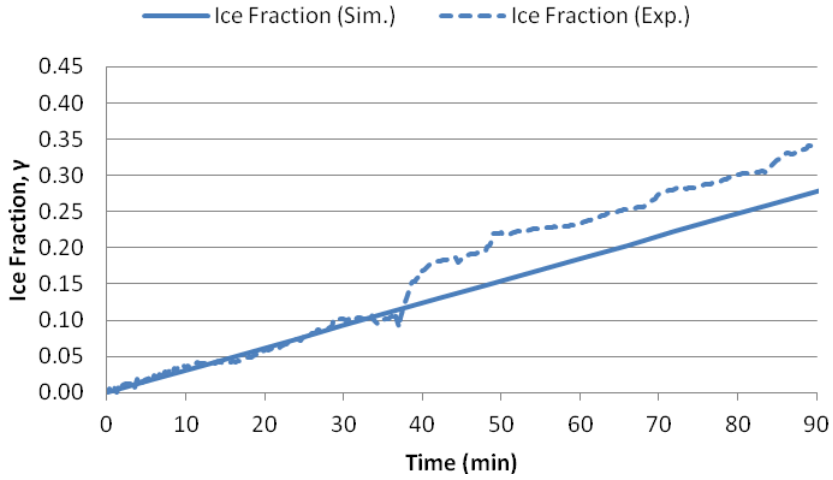

Figure 4- Simulated and Experimental Ice Fraction for Charging Process

Figure 5 compares the simulated and experimental tank fluid temperature. Again, both data sets are quite similar, with a slow decrease in fluid temperatures as ice builds in the tank. The maximum discrepancy between the two sets of data is 0.30°C.

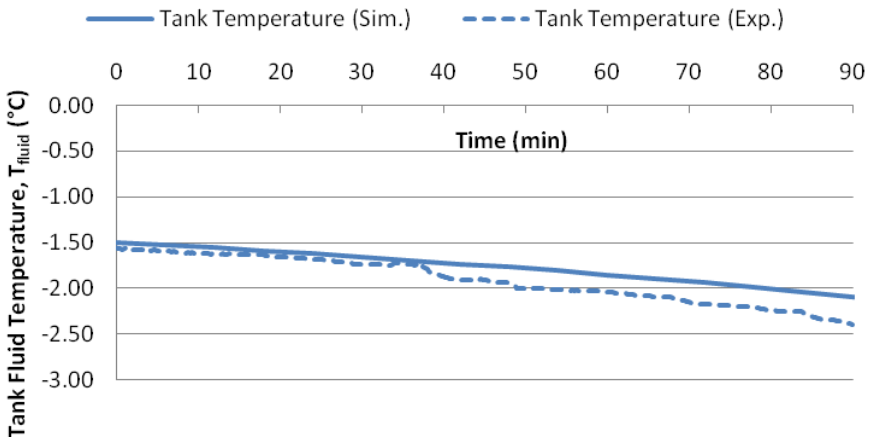

Figure 5- Simulated and Experimental Tank Fluid Temperature for Charging Process

Validation of the Discharging (Ice Melting) Process

The performance of the ice tank model in the discharge mode was validated using two sets of data from ASHRAE RP707 (ASHRAE, 1993). This test report was selected as it provided data for the uniform distribution of inlet flow over the top of the tank as assumed by the mathematical model (The ice slurry test bench at the CanmetENERGY facility had a single inlet opening in the side of the tank, and thus was unable to provide test data for a uniformly distributed inlet water flow). It is important to note that the two test cases used during the validation process are different from those used during the development of the effectiveness function.

Experimental data in the report is provided for a rectangular tank (2.44m by 1.22m, with a height of 1.22m) operating using pure water as the working fluid. For each test case, water was extracted from the bottom of the ice tank and passed to an electrical heating vessel used to simulate a thermal load. A nozzle was then used to uniformly distribute inlet water over the top of the ice layer, while type T thermocouples at the nozzle and outlet of the tank were used to measure the inlet and outlet fluid temperatures.

A summary of the key test parameters is provided in Table 1. It was assumed that all inlet fluid entered directly from the heating vessel, with no additional contributions from the heat pump/ice generator.

Table 1- Test Parameters for Validation of Discharge Process (ASHRAE, 1993)

	Run	
Test Parameters	**1**	**2**
Initial Ice Mass, m_{ice}^{0} (kg)	1205	1499
Initial Fluid Temperature, T_{fluid}^{0} (°C)	0	0
Inlet Fluid Flow Rate, $\dot{m}_{col}$ (kg/h)	0.758	0.758
Inlet Fluid Flow Temperature, $T_{o,col}$ (°C)	7.8	19.4

Figure 6 compares the simulated and experimental ice fractions (by mass) for Test Run #1, while Figure 7 shows the same information for Test Run #2. In each case, the simulated and experimental data follow a similar trend, with a steady decrease in the ice fraction over time. The maximum discrepancy between the simulated and experimental results is 3% of the tank storage capacity for Test Run #1, and 1% of the tank storage capacity for Test Run #2.

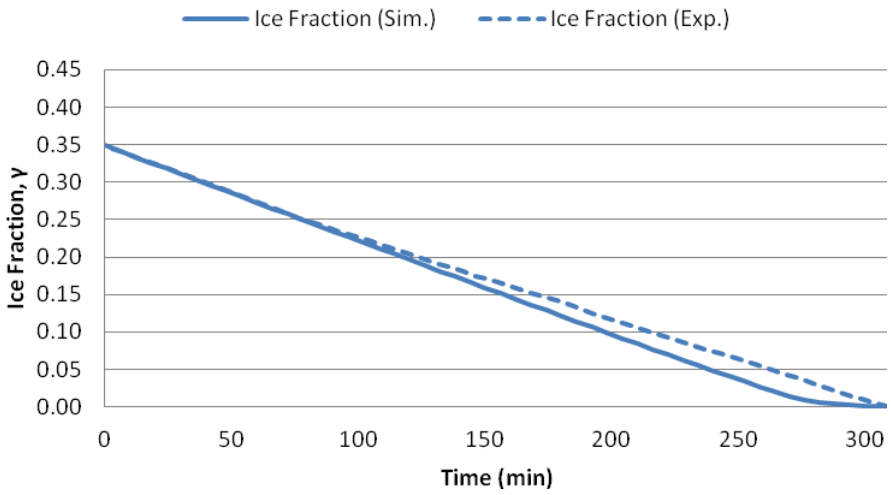

Figure 6- Simulated and Experimental Ice Fraction for Test Run #1

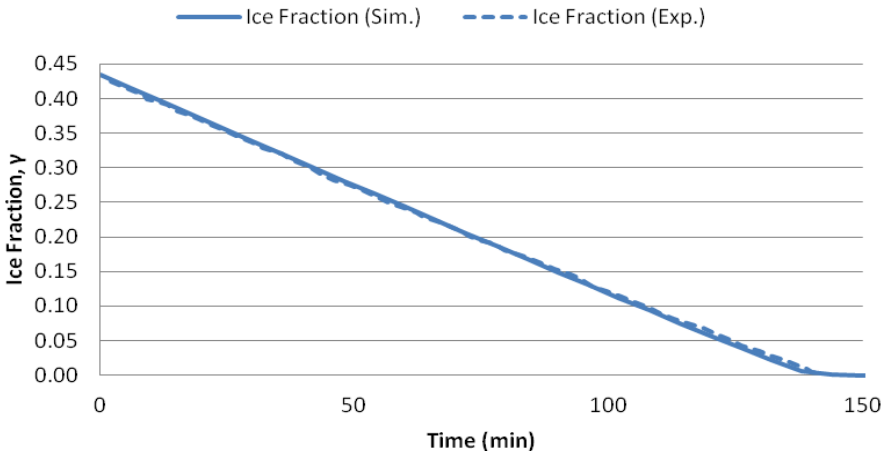

Figure 7- Simulated and Experimental Ice Fraction for Test Run #2

Figure 8 compares the simulated and experimental tank fluid temperature for Test Run #1, while Figure 9 shows the same comparison for Test Run #2. The developed ice tank model is able to match the general trend of a slow fluid temperature rise at high ice fractions, followed by a more rapid increase in fluid temperatures as the ice fraction approaches zero. The maximum discrepancy between the simulated and experimental data is 0.75ºC for Test Run #1, and 3ºC for Test Run #2. One potential source of these discrepancies is the location of the thermocouples used to measure the tank fluid temperature: The temperatures provided in RP707 were measured at the perimeter outlet of the tank, and may not be fully representative of the average tank fluid temperature calculated by the ice tank model. In addition, the accuracy of the type T thermocouples used for the temperature measurements is ± 1°C, which could also contribute to the discrepancy between the two data sets.

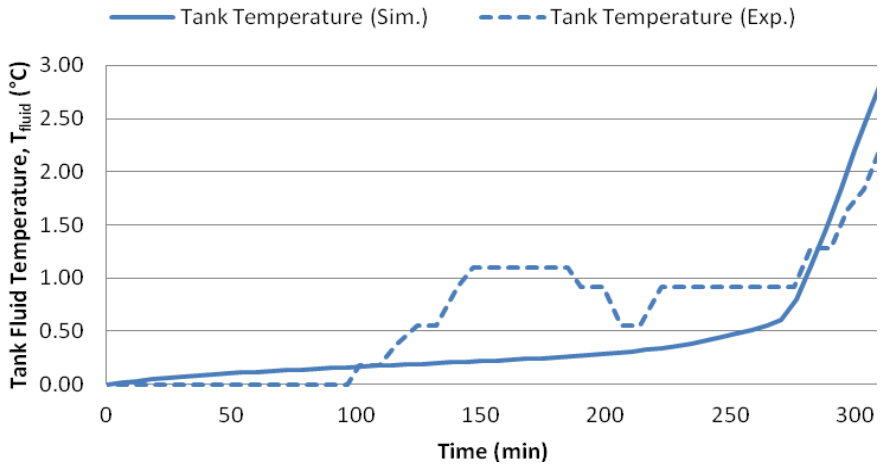

Figure 8-Simulated and Experimental Tank Fluid Temperature for Test Run #1

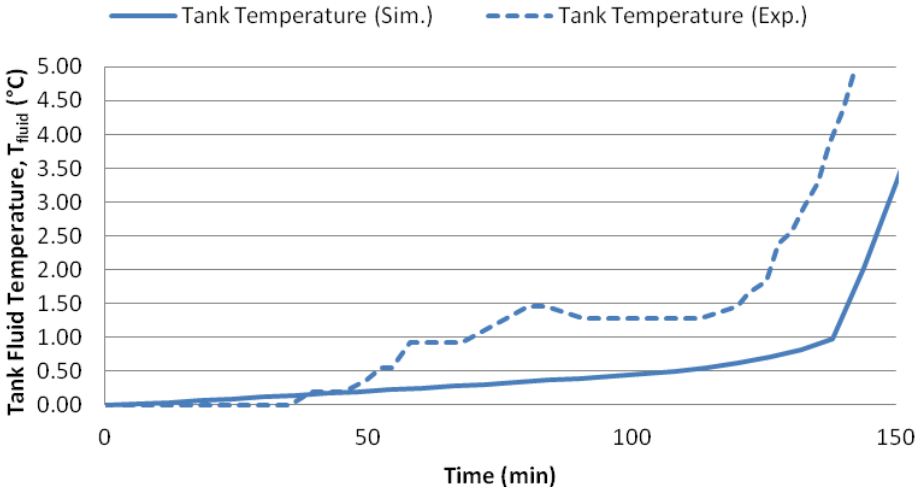

Figure 9- Simulated and Experimental Tank Fluid Temperature for Test Run #2

5 Conclusion

Ice slurry offers a number of potential advantages when applied to solar assisted heat pump systems. However, its proper design and integration into the built environment requires the ability to accurately and efficiently simulate the performance of the storage tank on a systems level. As such, a new mathematical model has been developed for a non-agitated ice slurry tank based on energy balance equations for the ice and water layers. Each of the defining equations was discretized, and used as the base for a new component model for the TRNSYS energy simulation program. A validation of the ice tank model showed the ability to adequately predict the ice mass and tank fluid temperature in both the ice building and ice melting modes of operation.

6 Acknowledgements

The authors acknowledge the financial support received from the Natural Sciences and Engineering Research Council of Canada, Natural Resources Canada/CanmetENERGY, and the Faculty of Engineering and Computer Science at Concordia University.

7 References

ASHRAE, 1993. Development of a Design Procedure for Thermal Energy Storage Tanks Which Separate the Manufacture from the Storage of Ice (Final Report Research Project 707). Atlanta: ASHRAE.

ASHRAE, 2007. *2007 ASHRAE Handbook:HVAC Applications*. Atlanta, GA: ASHRAE.

Behschnitt, S. A., 1996. A Comparison of Water-Ethanol, Pure Water and Ice as Storage Media for Building Thermal Storage Applications (M.S Thesis, University of Wisconsin-Madison). Available at: http://minds.wisconsin.edu/handle/1793/39136?show=full [Accessed Dec. 1, 2009].

Egolf, P.W, Kitanovski, A., Ata-Cesar, D., Vuarnoz, D., & Meili, F. , 2008. Cold storage with ice slurries. International Journal of Energy Research, 32(3), 187-203.

Freeman, T.L, Mitchell, J.W., & Audit, T.E., 1978. Performance of combined solar-heat pump systems. Solar Energy, 22(2), 125-135.

Hasnain, S., 1998. Review on sustainable thermal energy storage technologies. II. Cool thermal storage. *Energy Conversion and Management*, *39*(11), 1139-1153.

Hawes, D.W., Feldman, D., & Banu D. , 1993. Latent heat storage in building materials. *Energy and Buildings*, *20*(1), 77-86.

IIR, 2005. Handbook on Ice Slurries-Fundamentals and Engineering. Paris:IIR/IIF.

Klein et al., 2004. TRNSYS 16 - A TRaNsient SYstem Simulation program, User manual. Getting Started — Solar Energy Laboratory, University of Wisconsin-Madison. For more information, see http://sel.me.wisc.edu/trnsys/default.htm

Renaud-Boivin, S., Poirier, M., and Galanis, N, 2012. Experimental Study of Hydraulic and Thermal Behaviour of an Ice Slurry in a Shell and Tube Heat Exchanger. *Experimental Thermal and Fluid Science*, *37* (February 2012), 130-141.

Tamasauskas, J., Poirier, M., Zmeureanu, R., & Sunye R, 2011. Concept and Performance of a Solar Assisted Heat Pump Using Ice Slurry as a Storage Medium. *In Proceedings of Climamed '11: VI Congreso Mediterraneo de Climatizacion*, Madrid.

Tanino, M., & Kozawa, Y., 2001. Ice-water two-phase flow behavior in ice heat storage systems. *International Journal of Refrigeration*, *24*(7), 639-651.

UNIPHIZ Lab., 2011. Findgraph V2.311. Available at: http://www.uniphiz.com/findgraph.htm [Accessed January 10, 2011].

Ure, Z., 1999. Slurry ice based cooling systems. *In Proceedings of 20th International Conference on Refrigeration into the Third Millenium,* Sydney.

8 Nomenclature

Symbols

A	Area (m^2)
IGR	Ice Generation Rate from Heat Pump (kg/s)
L	Latent Heat of Ice (333550 J/kg)
T	Temperature (°C)
U	Tank Loss Coefficient ($W/m^2°C$)
c_p	Specific Heat of Fluid in the Ice Tank (J/kg)
h	Convection Heat Transfer Coefficient ($W/m^2°C$)
m	Mass (kg)
t	time (s)

Greek Symbols

ε	Effectiveness coefficient (-)
$\dot{m}$	Fluid mass flow rate (kg/s)
η	Solar collector efficiency (-)
λ	Ethylene glycol mass concentration (-)
γ	Ice mass fraction (-)

Subscripts and Superscripts

0	Initial
HP	Heat pump
amb	Outdoor ambient
c	Contact area between water and ice layers
col	Collector
env	Room Environment
fluid	Fluid layer
gly	Glycol
i	In
ice	Ice layer
n	Iteration number
o	Out
s	Surface area exposed to tank wall
t	Time step *t*
tank	Total ice tank